NAVAL POSTGRADUATE SCHOOL

MONTEREY, CALIFORNIA

THESIS

DECADAL FRESHENING AND WARMING OF THE
WESTERN ARCTIC UPPER OCEAN

by

Russell G. Ingersoll

September 2010

Thesis Advisor:	Timothy P. Stanton
Second Reader:	William J. Shaw

Approved for public release; distribution is unlimited

THIS PAGE INTENTIONALLY LEFT BLANK

REPORT DOCUMENTATION PAGE		Form Approved OMB No. 0704-0188

Public reporting burden for this collection of information is estimated to average 1 hour per response, including the time for reviewing instruction, searching existing data sources, gathering and maintaining the data needed, and completing and reviewing the collection of information. Send comments regarding this burden estimate or any other aspect of this collection of information, including suggestions for reducing this burden, to Washington headquarters Services, Directorate for Information Operations and Reports, 1215 Jefferson Davis Highway, Suite 1204, Arlington, VA 22202-4302, and to the Office of Management and Budget, Paperwork Reduction Project (0704-0188) Washington DC 20503.

1. AGENCY USE ONLY (Leave blank)	2. REPORT DATE September 2010	3. REPORT TYPE AND DATES COVERED Master's Thesis
4. TITLE AND SUBTITLE Decadal Freshening and Warming of the Western Arctic Upper Ocean.		**5. FUNDING NUMBERS** N/A
6. AUTHOR(S) Russell G. Ingersoll		

7. PERFORMING ORGANIZATION NAME(S) AND ADDRESS(ES)
   Naval Postgraduate School
   Monterey, CA 93943-5000
		8. PERFORMING ORGANIZATION REPORT NUMBER
		N/A

9. SPONSORING /MONITORING AGENCY NAME(S) AND ADDRESS(ES) N/A		**10. SPONSORING/MONITORING AGENCY REPORT NUMBER** N/A

11. SUPPLEMENTARY NOTES The views expressed in this thesis are those of the author and do not reflect the official policy or position of the Department of Defense or the U.S. Government. IRB Protocol Number _____N/A_____

12a. DISTRIBUTION / AVAILABILITY STATEMENT Approved for public release; distribution is unlimited	12b. DISTRIBUTION CODE UU

13. ABSTRACT (maximum 200 words)

Upper-ocean freshness and heat content are important components of the coupled Arctic system, especially within the context on ongoing Arctic change. High resolution hydrographic profile data collected from Arctic research expeditions and autonomous systems are analyzed to generate a 30+ year record of upper-ocean fresh water content and heat content evolution. Vertical integrals of Heat Content (HC) and Fresh Water Content (FWC) are calculated in three layers: Surface(Sfc)-150m, Sfc-Mixed Layer Depth (MLD), and MLD-150m. Vertical averages of Departure From Freezing Point (DFFP), Salinity(z), and Temperature(z) are also calculated for all three layers. Spatial and temporal constraints allow for seasonal and regional signals to be separated from decadal trend signals. Sub-regions (Beaufort Shelf, Beaufort Gyre, and Trans-polar Drift) are chosen with respect to hydrographically uniform characteristics. In the Beaufort Gyre, Sfc-150m vertically averaged salinity decreases by -0.04 psu/yr while FWC increases by +0.15 m/yr, and HC rises by +3.8 MJ/m^2/yr. Mixed layer vs. Halocline trend separation (Sfc-MLD vs. MLD-150m) shows accumulation of FWC in both layers definitively, while the halocline hosts almost all of the accumulation of HC. The trends in FWC are consistent with the observed decline in Arctic sea ice cover.

14. SUBJECT TERMS Arctic Ocean, Mixed Layer, Halocline, Fresh Water Content, Heat Content, Temperature, Salinity, Departure From Freezing Point, Canada Basin, Beaufort Gyre, Beaufort Shelf, Trans Polar Drift.			**15. NUMBER OF PAGES** 63
			16. PRICE CODE
17. SECURITY CLASSIFICATION OF REPORT Unclassified	**18. SECURITY CLASSIFICATION OF THIS PAGE** Unclassified	**19. SECURITY CLASSIFICATION OF ABSTRACT** Unclassified	**20. LIMITATION OF ABSTRACT** UU

NSN 7540-01-280-5500

Standard Form 298 (Rev. 2-89)
Prescribed by ANSI Std. 239-18

i

THIS PAGE INTENTIONALLY LEFT BLANK

DECADAL FRESHENING AND WARMING OF THE WESTERN ARCTIC UPPER OCEAN

Russell G. Ingersoll
Lieutenant, United States Navy
B.A., University of Colorado, Boulder, 1994

Submitted in partial fulfillment of the
requirements for the degree of

MASTER OF SCIENCE IN METEOROLOGY AND PHYSICAL OCEANOGRAPHY

from the

**NAVAL POSTGRADUATE SCHOOL
September 2010**

Author: Russell G. Ingersoll

Approved by: Timothy P. Stanton
Thesis Advisor

William J. Shaw
Second Reader

Jeffrey D. Paduan
Chairman, Department of Oceanography

iii

THIS PAGE INTENTIONALLY LEFT BLANK

ABSTRACT

Upper-ocean freshness and heat content are important components of the coupled Arctic system, especially within the context on ongoing Arctic change. High resolution hydrographic profile data collected from Arctic research expeditions and autonomous systems are analyzed to generate a 30+ year record of upper-ocean fresh water content and heat content evolution. Vertical integrals of Heat Content (HC) and Fresh Water Content (FWC) are calculated in three layers: Surface(Sfc)-150m, Sfc-Mixed Layer Depth (MLD), and MLD-150m. Vertical averages of Departure From Freezing Point (DFFP), Salinity(z), and Temperature(z) are also calculated for all three layers. Spatial and temporal constraints allow for seasonal and regional signals to be separated from decadal trend signals. Sub-regions (Beaufort Shelf, Beaufort Gyre, and Trans-polar Drift) are chosen with respect to hydrographically uniform characteristics. In the Beaufort Gyre, Sfc-150m vertically averaged salinity decreases by -0.04 psu/yr while FWC increases by +0.15 m/yr, and HC rises by +3.8 MJ/m^2/yr. Mixed layer vs. Halocline trend separation (Sfc-MLD vs. MLD-150m) shows accumulation of FWC in both layers definitively, while the halocline hosts almost all of the accumulation of HC. The trends in FWC are consistent with the observed decline in Arctic sea ice cover.

THIS PAGE INTENTIONALLY LEFT BLANK

TABLE OF CONTENTS

THIS PAGE INTENTIONALLY LEFT BLANK

LIST OF FIGURES

x

LIST OF TABLES

THIS PAGE INTENTIONALLY LEFT BLANK

LIST OF ACRONYMS AND ABBREVIATIONS

AFL   Albedo Feedback Loop

AIDJEX   Arctic Ice Dynamics Joint Experiment

APLIS   Applied Physics Laboratory Ice Station

BG   Beaufort Gyre

CNO   Chief of Naval Operations

CTD   Conductivity-Temperature-Depth

DFFP   Departure From Freezing Point

deg C   Degrees Centigrade

FWC   Fresh Water Content

HC   Heat Content

ITP   Ice Tethered Profiler

MJ   Megajoules

ML   Mixed Layer

MLD   Mixed Layer Depth

MLDS   Mixed Layer Depth Salinity

MLDT   Mixed Layer Depth Temperature

MLS   Mixed Layer Salinity

MYI   Multi-Year Ice

NaN   Not a Number

NAR   Navy Arctic Roadmap

NCCR   Navy Climate Change Roadmap

NPS   Naval Postgraduate School

NSIDC   National Snow and Ice Data Center

NSPD-66   National Security Presidential Directive 66

ONR   Office of Naval Research

psu   Practical Salinity Unit(s)

SHEBA   Surface Heat Budget of the Arctic

TFCC   Task Force Climate Change

WHOI   Woods Hole Oceanographic Institute

THIS PAGE INTENTIONALLY LEFT BLANK

ACKNOWLEDGMENTS

THIS PAGE INTENTIONALLY LEFT BLANK

I. INTRODUCTION

A. MOTIVATION

Widespread changes in the coupled Arctic ocean/ice/atmosphere system have been observed in the last decade. In response to these changes, National Security Presidential Directive 66 (NSPD-66), of January 2009, establishes that the U.S. Department of Homeland Security and Department of Defense will cooperatively implement new objectives for the Arctic region: enhancing cooperation among Arctic stake-holders (inter-agency and/or inter-governmental), maintaining safety and security, protecting its fragile environment and abundant natural resources, and promoting increased scientific monitoring (NSPD-66 2009). Specific to the Navy, the newly established Task Force Climate Change (TFCC) was created in the summer of 2009 as directed by the Chief of Naval Operations (CNO), and it serves as the primary advisory entity for Arctic related and climate-change related naval planning (TFCC 2009). TFCC is headed by the Oceanographer of the Navy. The *Navy Arctic Roadmap* (NAR), and *Navy Climate Change Roadmap* (NCCR) were delivered to the CNO by TFCC during its first year, and both documents invoke guidance from NSPD-66.

In view of climate change evidence and these recent policies, there is a growing need for improved understanding of the Arctic environment. This promotes a growing level of interest and support for observational and theoretical studies. The Arctic Ocean is an important component of the whole Arctic system and is the focus of this study.

B. OBJECTIVES AND KEY TERMS

The main purpose of this study is to investigate multi-decadal freshening and warming trends through analysis of a 30+ year compilation of high-resolution Conductivity-Temperature-Depth (CTD) profile data from the western Arctic. Emphasis is placed on the upper 150 meters (m) of the southern Canada Basin and Beaufort Gyre, with comparison to the Beaufort Shelf and the Central Arctic (Trans Polar Drift) regions. The results will be discussed with respect to relationships to sea ice transformation, advection through the Bering Strait, and river runoff.

Seawater properties discussed include upper-ocean salinity (S), temperature (T), Fresh Water Content (FWC), Departure From Freezing Point (DFFP), and Heat Content (HC). FWC in this paper specifically implies the liquid fresh water in the column, excluding the fresh water held within sea ice. The structure of the water column is discussed in terms of changes in S and/or T with depth, where-by the Mixed Layer (ML), Mixed Layer Depth (MLD), and Mixed Layer Salinity (MLS) are identified. Depth is expressed in meters (m). The primary challenge is to evaluate these measures of freshness and heat by computer-based statistical analysis that isolate the signals of long term (decadal) evolution from seasonal and spatial variabilities.

Additional key terms, expeditions, and organizations relevant to this discussion are: Naval Postgraduate School (NPS), Applied Physics Laboratory Ice Station (APLIS), Arctic Ice Dynamics Joint Experiment (AIDJEX), Surface Heat Budget of the Arctic Ocean Project (SHEBA), Woods Hole Oceanographic Institute (WHOI), Ice Tethered Profilers (ITPs), and National Snow and Ice Data Center (NSIDC). The acronym NPS10 is used in reference to this study as a whole, or with respect to sub-sections of this experiment when being compared to related/relevant works.

II.   BACKGROUND

A.   RECENT OBSERVATIONS OF ARCTIC CHANGE

Studies conducted in recent years have shown temporal trends in the hydrography of the Arctic upper ocean. An important example is the examination of sea water freshness in the Western Arctic by McPhee et al. (1998) after the SHEBA expedition in the late 90s. This analysis compared AIDJEX profiles from the mid-70s to the SHEBA profiles. This provided a unique opportunity to compare high resolution observations some 20 years apart from very similar locations, and the results showed the more recent data had upper ocean salinities markedly less than the 70s data set. More specifically, the "salinity deficit in the upper 100m" shown by this comparison indicates a fresh water "equivalent thickness input" of approximately two meters over the two decades. An increase in melt rate for Arctic sea ice was conjectured as a dominant contribution to the observed freshening effect.

Stroeve et al. (2007) examined climate model performances and sea ice extent observations to assess the relationship of model skill to actual sea ice evolution. This experiment finds that "from 1953–2006, Arctic sea ice extent, at the end of the melt season, has declined at a rate of -7.8% per decade," while the trend during the satellite era (1979–2006) has a steeper decline rate of -9.1% per decade. It is also emphasized in this discussion that there is "near universal agreement" among climate models that Arctic sea ice will continue to decline through the current century, and that the shared roles of "natural variability" and "forced change" (by loading the atmosphere with *Green House Gases*) need to each be considered as key contributors to the trend. Figure 1 illustrates the disparity between climate model forecasts and the observational record.
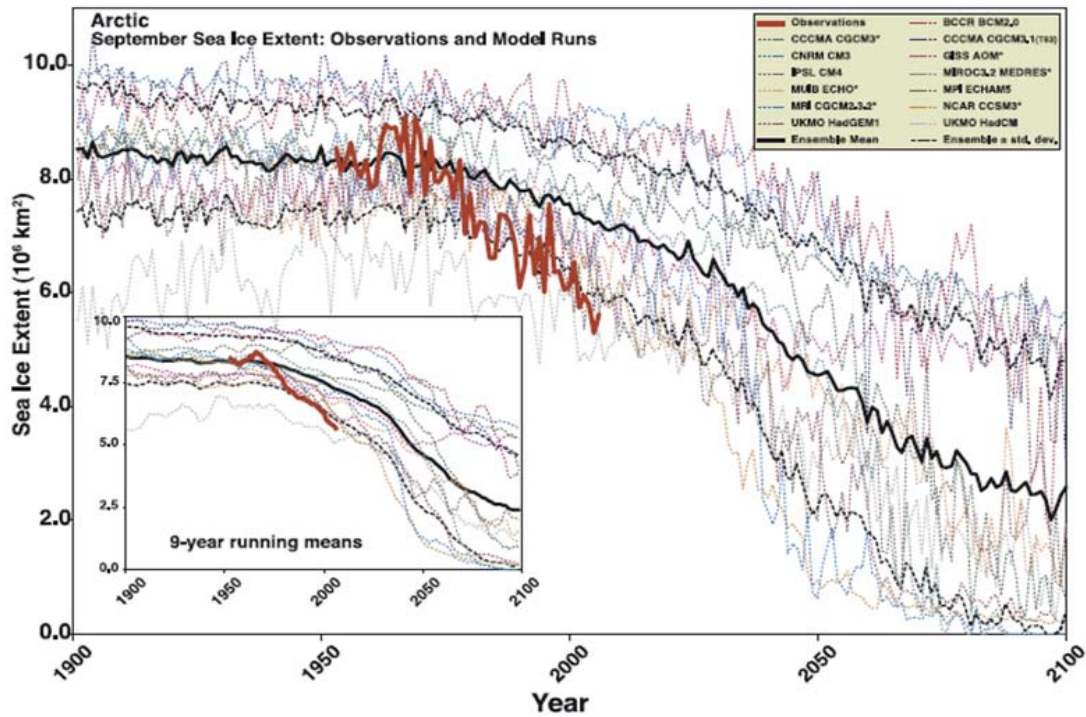
Figure 1.   Arctic September Sea Ice Extent from observations (thick red line) and 13 climate models, together with the multi-model ensemble mean (solid black line) and standard deviations (dotted black lines) (From Stroeve et al. 2007).

B.   DRIVERS OF ARCTIC UPPER OCEAN CHANGE

Arctic upper-ocean freshness and heat are influenced by several factors. The Arctic system as a whole is coupled, where-by the influences of the atmosphere and ocean acting on the ice cover allow the system to sustain (or not sustain) long term perennial ice cover through extreme seasonal changes in surface forcing. A critical phenomenon acting as a driver of change in the Arctic is the sea ice Albedo Feedback Loop (AFL). In the upper ocean, this acts as a driver of change with respect to both freshening and warming.

1.   Albedo Feedback Loop (AFL)

Albedo is a measure of the reflective ability of any given surface material. Ice cover and/or snow cover have the highest albedo of any naturally occurring surface on earth (Laine 2004). In winter, maximum sea ice cover together with maximum coverage

of the ice by snow results in approximately 80–90% albedo over the Arctic region, while the albedo of an ice free ocean surface can be as low as 4% (Hanson 1961). To visualize the importance of the AFL, consider a theoretical polar environment in a state of interannual equilibrium. The same amount of snow would accumulate on the land and sea ice surfaces each winter, then melt away at the same rate each summer, and so forth in the following seasons. Also, the same amount of sea ice would accumulate (by freezing) so as to cover the same amount of ocean surface each winter, then melt away to the same minimum coverage each summer, before repeating the cycle. Under these circumstances, there would be no interannual net change in the average reflective properties, as caused by the snow and ice, of the Arctic surface. With other relevant factors in equilibrium as well, e.g., cloudiness, and radiation intensity, the region would have a balanced budget indefinitely with respect to the absorption vs. reflection of solar energy. As the albedo of sea water is less than sea ice, which is less than snow (Hanson 1961), sea water is the best absorber. Now consider the observed trend of decreasing sea ice over recent decades juxtaposed with an increase in the average amount of exposed ocean. Over the past 30 years, there has been an approximate increase in the length of the "melt season" by ~20 days (Markus et al. 2009), and total amount of solar heat absorption within a given season is linked to the start-time of the melt season (Perovich et al. 2007), which has become slightly earlier than normal. While the loss of ice augments the melt season and allows the seawater to absorb greater amounts of solar energy during each successive year, the pattern forms a positive feedback loop with the increased summer heating inhibiting the formation of ice the following fall. The AFL could work in the opposite direction just as well; however, the current direction of this feedback contributes to the decline of sea ice, where-by the melt water contributes to increased freshness (Yamamoto-Kawai et al. 2009), and the thinness of the ice, along with more exposed ocean, contributes to increased transmission of solar energy into the water (Perovich 2005).

2.   Freshening Effects

Contributions to freshness of the Arctic upper ocean are made by advection, river-runoff/precipitation, and melt water from sea ice (McPhee et al. 2009; Serreze et al. 2006; Yamamoto- Kawai et al. 2009). It makes intuitive sense that sea ice transformation will affect the salinity of the water in immediate proximity to the ice. As new ice is freezing (forming) the brine rejection process increases the salinity of the water below (Ekwurzel et al. 2001), while the melting of ice adds newly liquefied fresh water and reduces the salinity once it is mixed into the column. The loss of ice extent as previously shown in Figure 1, is complimented by observed loss in thickness. A recent examination of upward looking sonar data provided by U.S. Navy submarines, along with remote sensing data, shows that the past 40+ years are marked by a thinning trend in the Western, Central and Eastern Arctic regions (Kwok 2009), as shown in Figure 2.
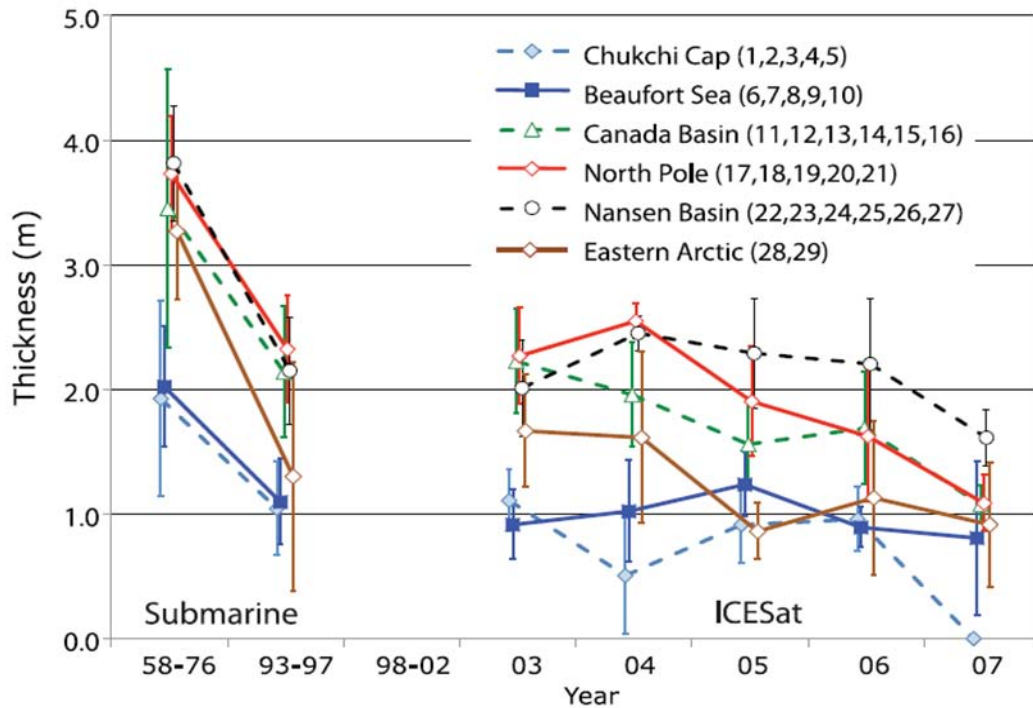
Figure 2.   Regional averages of Arctic sea ice thickness based on upward looking sonar and satellite records (From from Kwok 2009).

Decreasing extent with decreasing thickness translates to loss in over-all ice volume. The loss in thickness is related to the average age of the ice. Recently, the presence of Multi-Year-Ice (MYI) has declined more rapidly than sea ice extent (Lindsay et al. 2008), as part of a transition to an Arctic sea ice cover that is dominated by first year ice, and consequently younger and thinner in the mean. In the past five years (considering the entire Arctic basin), the MYI coverage has been reduced by ~42% (Kwok et al. 2009). The new, thinner ice lends itself to melting more readily than older/thicker ice, further assisting the influence of the AFL. Younger ice is also more prone to transport by wind stress, and can potentially be moved out of the basin more easily (Lindsay et al. 2008), then melt in non-Arctic waters in the North Atlantic. Wind-driven export to the North Atlantic happens to MYI as well. Chemical analysis of a 5-year span of water samples in the Canada Basin (2003-2007) shows that melt water from sea ice was greater in 2006/07 (Yamamoto-Kawai et al. 2009), so the freshening contribution represented by sea ice transformation will become increasingly important if sea ice continues to decline at such fast rates.

Input of fresh water to the Arctic Ocean from river runoff is another contribution to the Arctic Ocean fresh water balance and most likely the largest (Arnell 2005; McPhee et al. 2009), as it provides approximately 38% of the annual average contribution (Serreze et al. 2006). To estimate this contribution, flow rates of major rivers and catchments in the Arctic hydrological system have been monitored for many years and data is periodically examined. As part of the National Science Foundation's Arctic System Science Program, Peterson and colleagues engaged in a multi-year investigation to "use river water chemistry as a means to study the origins and fates of continental runoff," revealing a 7% increase in discharge from six major Eurasian rivers, Figure 3, from the mid-30s to the late 90s (Peterson et al. 2002).
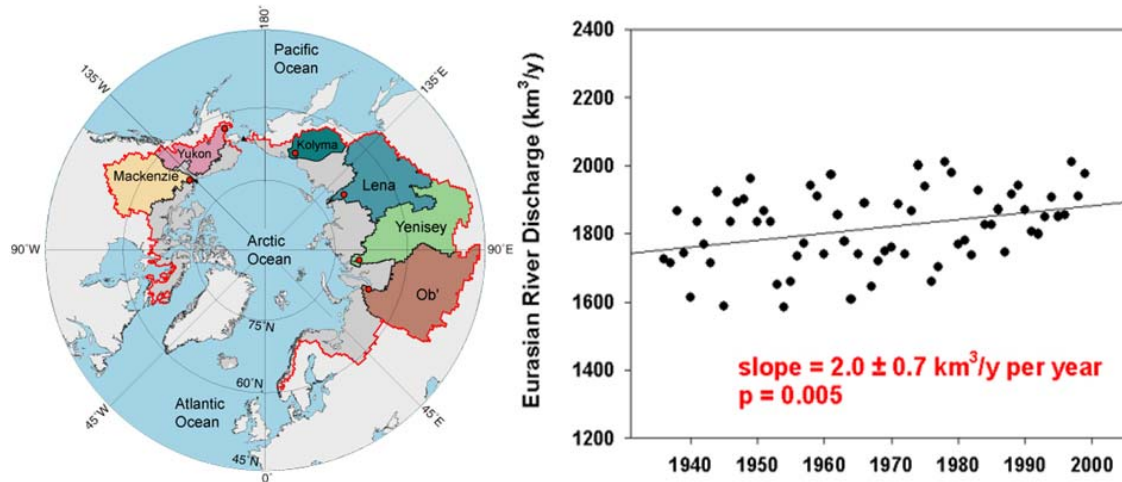
Figure 3.   Combined discharge of the six largest Eurasian rivers (Yenisey, Ob, Lena, Kolyma, Pechora, and Severnaya Dvina). Over the period of record (1936-1999), combined discharge has increased 7% (128 km^3/yr). (From Peterson et al. 2002).

Advected fresh water from water masses outside the Arctic Basin is also substantial (McPhee et al. 2009), and it represents ~30% of the annual fresh water input (Serreze et al. 2006) to the Arctic system. Relatively fresh, Pacific origin water enters the Western Arctic ocean via the Bering Strait. Some of this water originates in a buoyancy-driven coastal current generated by Alaskan river runoff. This water follows the Western Alaskan coastline pole-ward through the Bering Strait, along the Eastern boundary of the Chukchi Sea, then beyond Point Barrow. Additionally, some open-ocean Pacific water flows pole-ward due to the pressure gradient that exists, in part due to differences in T and S, between these major basins (Serreze et al. 2006). This flow passes through the Aleutian Islands and continues under the steering influences of the Bering shelf northward through the Bering Strait into the Chukchi Sea.

3.   Warming Effects

Other than the AFL, the advection of comparatively warm Pacific water into the Arctic through the Bering Strait is the other major influence on Heat Content in the upper Arctic Ocean. The heat energy moving northward from the Pacific can be substantial. Following the record low summer minimum of Arctic sea ice extent in 2007, a study was

conducted by Woodgate et al. (2010) to examine Bering Strait heat transport in years leading up to the event. It was found that the 2001 heat flux increased to nearly double by the time it reached a 2007 maximum of $5\text{-}6x10^{20}$ J/yr. Woodgate et al. suggest that this surge of advected heat may have played an important role in the amount of sea ice melt that occurred in that unusual season. The physical means of carrying this heat by the currents was discussed above.

THIS PAGE INTENTIONALLY LEFT BLANK

III. HIGH RESOLUTION CTD ARCHIVE

A. SOURCES

Hydrographic profile data for this study were compiled from Naval Postgraduate School (NPS) field work at the 2009 Applied Physics Laboratory Ice Station (APLIS) and from publically available high resolution data sets from other camps, expeditions and cruises since the 1970s: Woods Hole Oceanographic Institute's Ice Tethered Profilers (ITPs), Surface Heat Budget of the Arctic Ocean Project (SHEBA), Arctic Ice Dynamics Joint Experiment (AIDJEX), and hydrographic survey data managed in the National Snow and Ice Data Center (NSIDC) CTD archives. Of the total 20,710 profiles utilized in this study, the majority were reported by ITPs (the most recent data), while AIDJEX and SHEBA provide archives upward of 1000 observations each (spanning approximately 1 year of field work in both cases), and the other sources, provide compliments of a few hundred observations.

In order to support the main goal of this study, date sets had to meet two essential criteria: (1) the mixed layer was resolved, and (2) the vertical resolution was high (less than 1m increments).

1. AIDJEX

Observations from all four of the AIDJEX camps (Big Bear, Blue Fox, Caribou, Snowbird) were obtained from data archives at the University of Washington Applied Physics Laboratory. The record has high resolution profiles from the spring of 1975 until the summer of 1976, and there are typically 1–3 observations per day.

2. NSIDC

Observations from the NSIDC, Beaufort Sea Cruises and Ice Stations CTD Data Set, were downloaded from their public archives. The cruises took place from the late 1970s to the late 1990s during mid-late winter over periods of 1–3 weeks on station near the Beaufort Shelf. High resolution profiles were taken 1–3 times per day at selected locations.

3. SHEBA

Data from SHEBA was acquired from the local archives at NPS. It was originally collected by the NPS Ocean Turbulence Group and colleagues during the year-long drifting ice camp. The data set includes 2–8 high-resolution profiles per day averaged down from over 27000 profiles in the time series, over a span of ~300 days, from October 1997 to October 1998, measured with a dual sensor SBE 911 plus CTD.

4. APLIS

APLIS 2009 was the most recent in a series of camps run as a joint effort between the University of Washington Applied Physics Laboratory and the U.S. Navy Arctic Submarine Laboratory. NPS participated in the 2009 camp for deployment of an Autonomous Ocean Flux Buoy, and to collect CTD and pH profile data for oceanographic research funded by the Office of Naval Research (ONR). NPS participation in APLIS 2009 provided an opportunity to study the acoustic effects of changes in Arctic Ocean pH, as discussed in Col (2010), and to generate an up-to-date hydrographic analysis of the upper ocean, as presented in this thesis. After initial set-up and instrument testing at the camp, an intensive CTD time-series was conducted for 36 hours. This was followed by daily casts for the two week duration of the camp. The camp was located near 73N 143W, in the Beaufort Gyre. A Sea-Bird, SBE 19 plus V2 was used to take the CTD observations. NPS collected 202 profiles in total, most to 230+ meters depth and some to 500+ meters (Col 2010). On station, the raw data were periodically downloaded from the instrument and converted to ASCII format with Sea-Bird processing software then archived on portable drives and returned to NPS for post-trip analysis. There are 1-3 high resolution observations per day, spanning two weeks in March.

5. WHOI ITPs

The Ice Tethered Profiler (ITP) observations were downloaded from the Woods Hole public access server, and archived locally. Original files are available such that each buoy's data can be extracted individually. Twenty-three ITPs have provided observations to date for the Canada Basin. Coverage from 2005–2010 is represented, and

there are 1–3 high resolution observations per day for the entire deployment (life-span) of each buoy. Figure 4 shows a diagram of the ITP system, and illustrates the general process of collecting hydrographic profile observations in the Arctic environment.
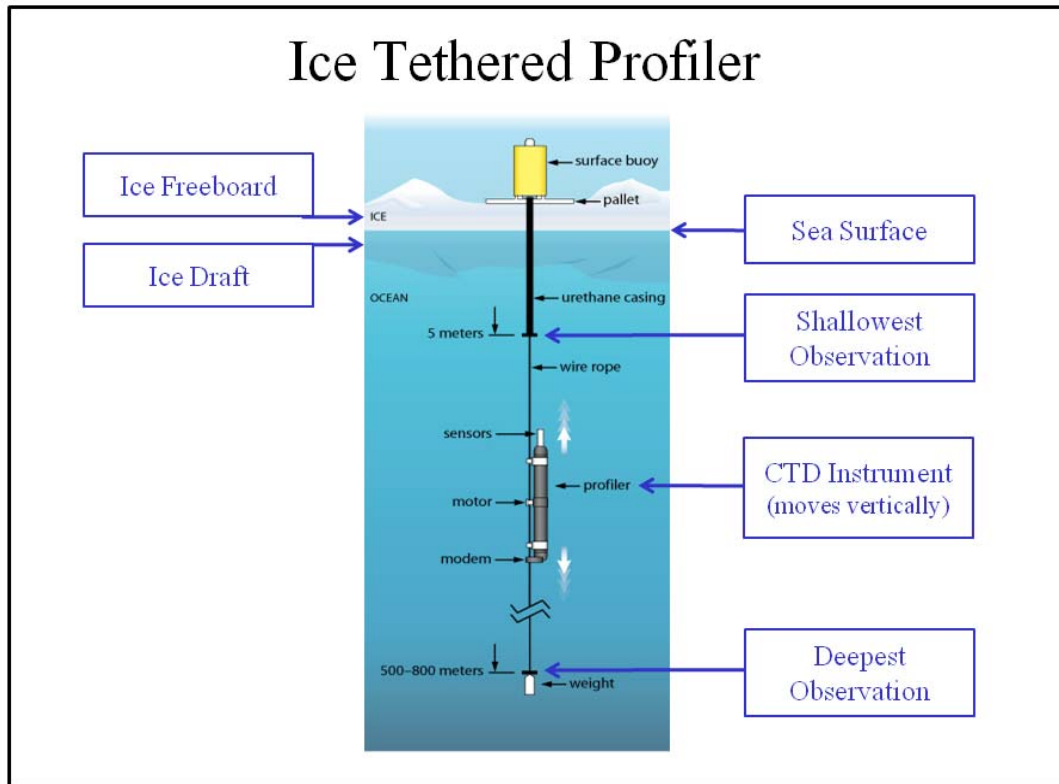
Figure 4.   Woods Hole Oceanographic Institute, Ice Tethered Profiler (ITP) system components. (From WHOI 2010).

THIS PAGE INTENTIONALLY LEFT BLANK

IV. METHODS

A. FORMING THE ARCHIVE

After collection from original sources, all data were processed into uniformly formatted matrices of vertical arrays of matching length ("the archive"). The archiving scripts interpolated the original S(z) and T(z) observations onto a depth vector of 1:500m, by 1m increments, then added each new vector to the archive. The interpolation scripts assigned the value "NaN" (not a number) to any depth bin where the original profile does not provide an observed value. Typically, this only occurs at the top and/or bottom portion of any given profile.

The APLIS and SHEBA data were originally recorded to depths of 150 to 200+ meters, so NaN was assigned to the remaining depths. NSIDC interpolation pre-screened the original profiles for casts of 150m or more for the archive, then discarded records that were too shallow. ITP and AIDJEX observations were generally very deep in original length and most provided a full 1:500m range of T and S for the archive.

B. SCREENING FOR BAD DATA

There are known vulnerabilities to CTD instruments, so all the CTD data sets were evaluated sensor malfunctions and glitches. A common cause of data errors was due to the interruption of the flow of seawater through the in-take port and conductivity sensor while the instrument is in its decent or ascent through the water column. This causes the conductivity sensor to have a slow response, generating significant errors in the salinity calculation. This and other intermittent issues can compromise some portion of, or all of an observation, and these profiles must be removed from the record to avoid unwanted effects on later calculations.

As mentioned, this study required profiles that resolve the mixed layer. In view of Figure 4, and the manner of most CTD observation methods, it is commonplace for profiles to have missing data near the very top of the column (near the surface). After

forming the archive, some profiles were missing data only for the upper-most few meters, while others were missing data for the top 10 or so meters of the water column, i.e., the degree to which the mixed layer was resolved was not consistent. From this point forward, "profiles" or "observations" are in reference to the matrix of interpolated arrays in the archive formed for this study, and are no longer referring to the original measurements in raw format.

1.   Manual Inspection

A cross-sectional, full-profile viewing script was used to look at multiple random samples of the archive, such that large portions of the archive could be examined after viewing multiple random sets consecutively. This allowed anomalies to be visually revealed, and scrutinized as to the reason for the anomalous vertical structure. In cases where the profile was deemed erroneous, a technique was derived to isolate any observations of the same nature, by automated methods.

2.   Automated Detection

Automated screening methods for each type of erroneous profile were applied, leaving only the good observations in the archive. When random samples no longer produced periodic erroneous profiles, it was deemed that the archive was usable for analysis of ocean structure.

C.   IDENTIFY THE MIXED LAYER DEPTH

Establishing the thickness of the mixed layer, or Mixed Layer Depth (MLD), was a critical step in this study, as the MLD defines the limits of many of the vertical integrals and vertical averaging calculations. These calculations can only be done when the profile is complete, e.g., when it contains observations from the surface to 150m without interruption. An initial step in this problem was to evaluate the differences in how much of the near-surface ocean was missing in the observations on a profile per profile basis. A variable called "first hit" was created to serve this purpose. It represents the earliest (shallowest) occurrence of an observed value of salinity (or temperature) for any given profile. In the case of ITP observations, the majority of first hits were at depths less than

or near 10 meters, although there were exceptions. First hits were also typically <10m for AIDJEX and SHEBA. In terms of the whole archive, the vast majority of first hits were at depths shallower than 20m. Profiles with first hits deeper than 20m were deemed as insufficiently resolving the mixed layer and were discarded. With proximity to the surface established by this general cut-off depth, the next step was to screen for sufficient consecutive observations occurring within the mixed portion of the water column. For this, all profiles were examined to ensure the presence of a minimum of 5 consecutive salinity observations such that all of 5 were within 0.2 psu of each other. By setting these criteria, profiles that resolved only a small portion of the mixed layer were discarded. Profiles with a definitive representation of the mixed layer (at least 5 observations; usually much more) were retained and passed into an index for further work. At this stage there was confident identification that the mixed layer is resolved within the remaining profiles, and other water column features could now be calculated: Locating the MLD, and extrapolation to the surface for S(z) and T(z).

The method of determining the base of the mixed layer relies on two fundamental assumptions: (1) the MLD will occur between 1m and 80m depth; determined by random sample viewing as discussed above, and (2) the largest vertical gradient the upper Halocline will be very near (below) the base of the mixed layer. Therefore, in this study the MLD is defined as the location of the maximum difference in consecutive S(z) within the first 80m, then upward by 2m. In Figure 5, the maximum difference in S(z) can clearly be seen as a "wide jump" just below the illustrated MLD. Visual inspection of multiple random samples of the archive confirmed consistent performance of this method in correctly identifying the top of the halocline in the vast majority of cases, thus correctly assigning MLD. With MLD determined, Mixed Layer Depth Salinity (MLDS) was assigned as the S(z) observed at MLD. The observed S(z) at the location of the first hit was assigned as Top Sal (TS). The group of observations between MLDS and TS were averaged to produce Mixed Layer Salinity (MLS). TS is then used as a recurring value for extrapolation to the surface. As each TS is unique to its own profile, it was only used for that profile. Figure 5, a salinity profile, illustrates the assignment of MLD and extrapolation to the surface with TS. Beginning with Mixed Layer Depth Temperature

(MLDT), an identical process was followed with respect to T(z) values in each profile, so as to generate all appropriate T related variables and surface extrapolation.
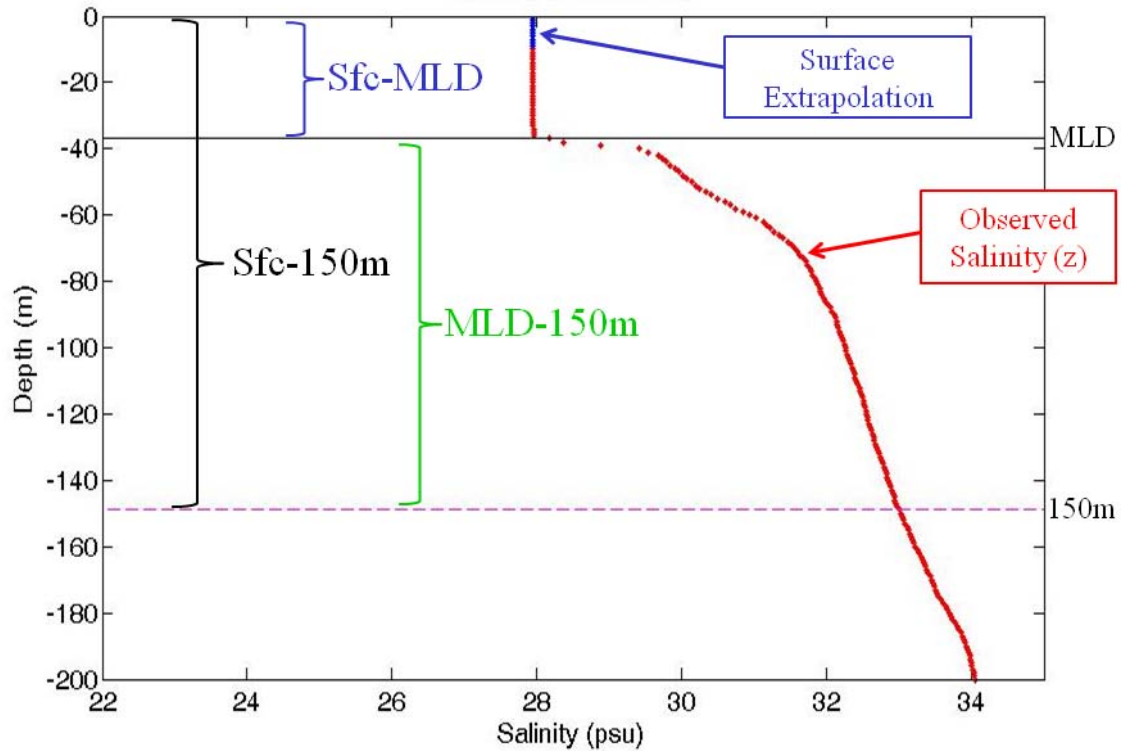
Figure 5.   Profile Cross-Section. Surface extrapolation shown in blue (at tope of profile). Typical example of Mixed Layer Depth identification (black horizontal line). Observed salinity(z) shown as red dotted line (traces change with depth and shows common Arctic salinity structure). Layer Calculations shown by color: Sfc-150m=Black, Sfc-MLD=Blue, MLD-150m=Green.

Nearly 20% of the archive did not meet the first five hits criteria and was not assigned an MLD numerically, while ~80% of the original archive were assigned an MLD and retained for use in the study.

D.   VERTICAL INTEGRALS

The study required examination of the water column through comparison of a combination of variables related to salinity and heat.   Two vertical integrals were calculated, Fresh Water Content (FWC) and Heat Content (HC).

FWC is evaluated by the equation:

$$FWC = \int_{Z2}^{Z1} \frac{Sref - S(z)}{Sref} dz \qquad (1)$$

Consider Figure 6 (left frame) with respect to application of the equation.   Sref (reference salinity) is set at 34.8 psu and remains unchanged for all layered calculations. Z1 is set at either the surface, or at MLD, and Z2 is set at either MLD or 150m.   FWC, expressed in meters, is evaluated for all three layers.   The expression of FWC in meters makes the assumption that the value represents a "fresh top" sitting on the ocean (or on top of the layer being calculated) with a thickness equivalent to the FWC calculation, while the remaining ocean below is imagined to be 34.8 psu entirely, as shown in Figure 6 (right frame).

HC relative to the in situ freezing point, determined by the local salinity and pressure, is evaluated by the equation:

$$HC = \rho Cp \int_{Z2}^{Z1} (T - Tfp) dz \qquad (2)$$

Similar to the FWC expression, Z1 and Z2 in the HC computation are adjusted per layer.   Density (ρ) is set at 1025 kg/m3.   Specific Heat (Cp) = 3850 J/(kg C).   The Freezing Point (Tfp) is salinity dependant, and adjusts in accordance with an embedded function.

19

Vertically averaged means are computed for all three layers for the remaining variables of interest: Salinity, Departure From Freezing Point, and Temperature. For all variables, the trend plot colors are consistent with the previously shown layer illustration in Figure 5.
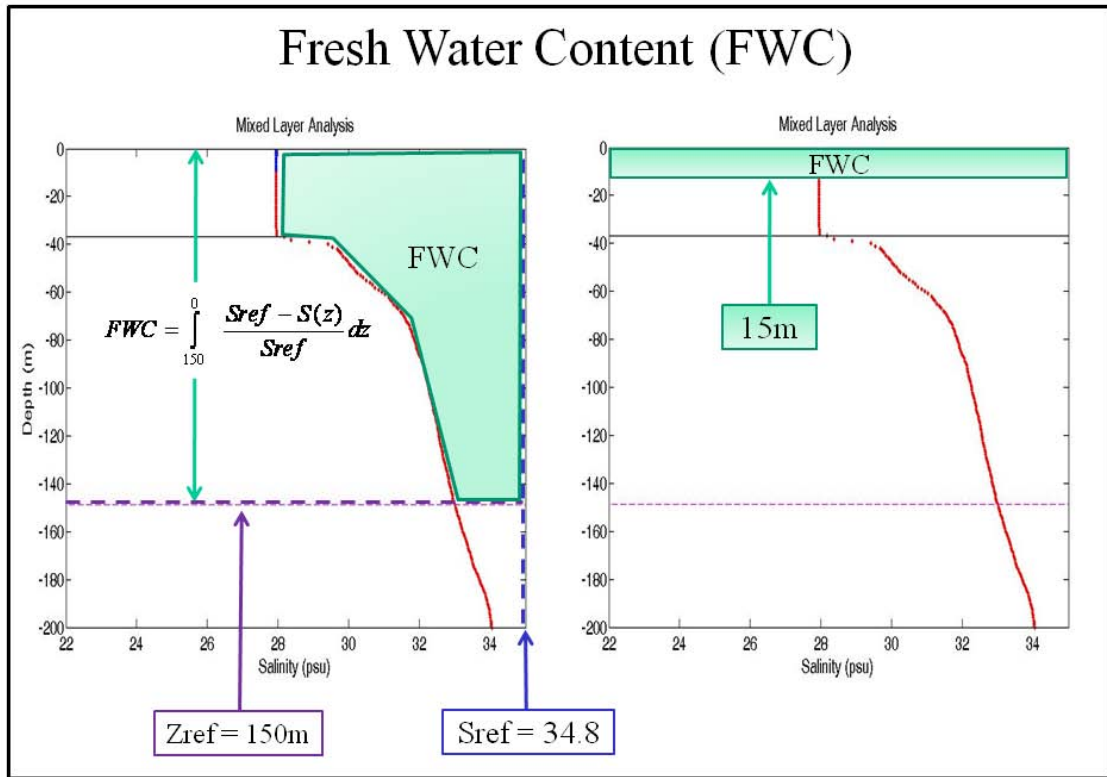
Figure 6. Fresh Water Content Illustration. Left panel shows formula for evaluating the FWC within any given vertical distance. Right panel shows the representation of FWC as expressed in meters (m). Zref is the Reference Depth (or Z2), and Sref is the Reference Salinity.

E. SPATIAL AND SEASONAL HOMOGENEITY

To look for a long-term signal in the data, measures were needed to reduce the variability introduced by spatial gradients. Therefore, homogenous sub-regions of the Western Arctic were needed so the study could be conducted on the basis of evaluating trends within areas of spatially uniform properties, then comparing the results of each area. The Mixed Layer Salinity (MLS) was utilized in this problem, along with general

knowledge of the Western Arctic Ocean as a system. For example, as a semi-permanent, anticyclonic circulation feature, the Beaufort Gyre is expected to have somewhat uniform properties within its perimeter.

It was also essential for this study to avoid seasonal variabilities and topographically induced influences that distort common water column structure. Time series analysis of the SHEBA data set, Figure 7, shows the benefit of constricting the analysis time window to a specific season. During Segment A, there tends to be fairly consistent structure on a day-by-day basis, and through many consecutive weeks. The SHEBA time series also illustrates the need to consider spatial variability – shortly after day 0 and again near day 25 there are spatial change signatures (ocean fronts or eddies) that affect the structure. Segments B and C, representing spring melt and mid-late summer respectively, both show a greater amount of short-term variability than the winter observations. Also of interest, after day 25, the SHEBA camp began to pass over a group of topographic features associated with the North Wind Rise/Ridge and the Chukchi Plateau, which also influenced the water column structure. The time window of December 1st to March 30th (here-after referred to as "wintertime") was chosen to reduce seasonal noise, while retaining a favorable sample size.
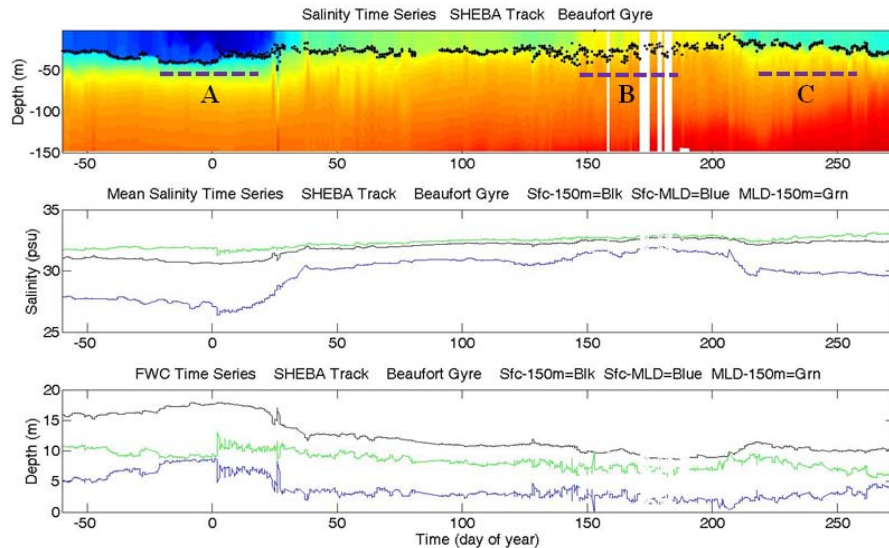
Figure 7. SHEBA Track Time Series of Salinity (Sfc-150m), 3-Layer Vertically Averaged Salinity, and 3-Layer Vertically Averaged Fresh Water Content.

21

By plotting the MLS of all wintertime observations, it was possible to visually identify homogenous sub-regions of the Western Arctic. As shown in Figure 8, the sub-regions chosen for this study are: The Beaufort Shelf, Beaufort Gyre (BG), and Central Arctic/Trans Polar Drift. For comparison within the gyre environment, the BG is evaluated with respect to the larger (green box) and smaller (red box) areas to see the effects on the following analyses when observations are restricted to a box just big enough to encompass the AIDJEX and SHEBA data sets, together with some recent ITPs. The depiction shows the general consistency of the MLS within each area, and that the sub-regions differ from each other markedly.
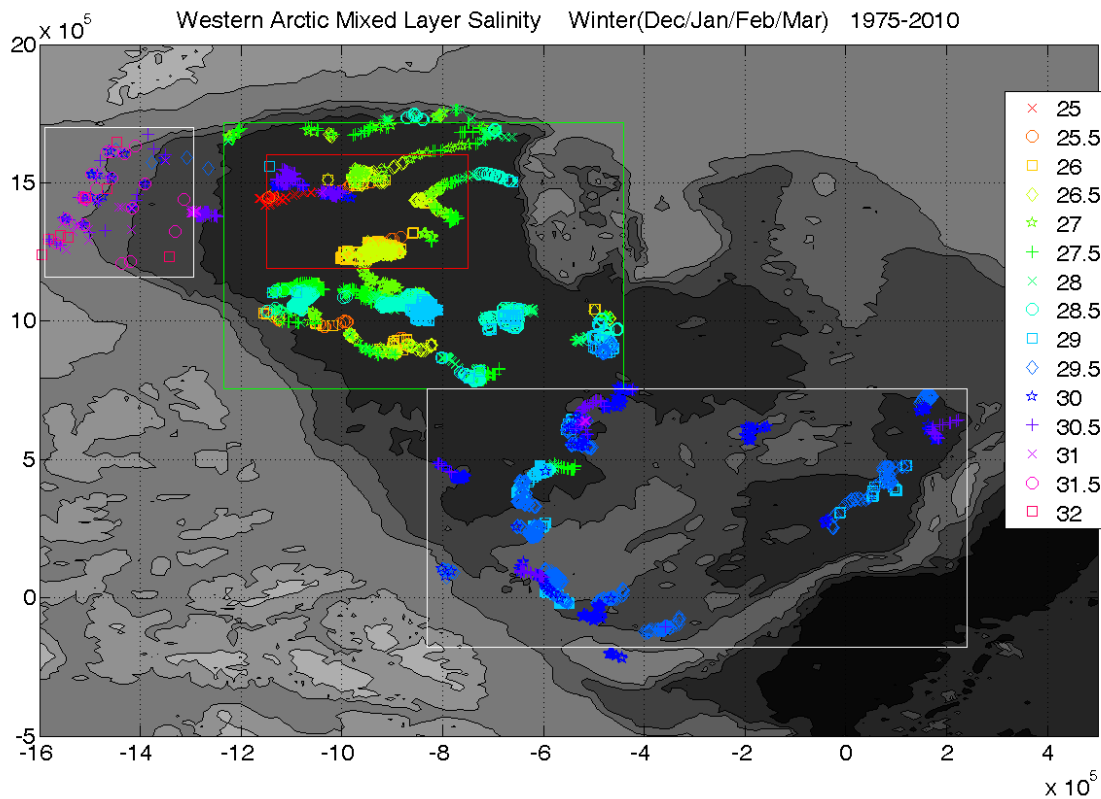
Figure 8.   Spatial and Seasonal homogeneity Plot: Comparison of Mixed Layer Salinity by Sub-region: Upper Left = Beaufort Shelf (White Outline), Upper Middle = Beaufort Gyre (Large) (Green Outline), Upper Middle In-set = Beaufort Gyre (Small) (Red Outline), and Lower Right = Trans Polar Drift (White Outline).

F.   ANALYSIS

Vertical Integrals and vertical averages were computed for all variables of interest and all three layers discussed in IV-D; this process was done separately for each of the homogenous sub-regions. In the case of the larger Beaufort Gyre sub-region, a greater number of total observations contribute to the estimates while there is a greater likelihood of variability introduced by spatial influences affecting the original measurements. In the case of the smaller Beaufort Gyre sub-region, the constricted distance between original measurements reduces the likelihood of spatial variability; however, a smaller number of observations is available to compute the estimates of the means. The Beaufort Shelf sub-region was sampled with much fewer original observations; however, many of the stations were re-visited (at the exact same locations) in sequential years.

THIS PAGE INTENTIONALLY LEFT BLANK

V. RESULTS

A. DECADAL TRENDS

For the Beaufort Shelf, a 16-year-long, wintertime record was analyzed, while the two Beaufort Gyre areas provided a 34-year-long, wintertime analysis. For each area (as defined and shown in Figure 8), trends over the period are depicted for each variable and for all three layers. This facilitates comparative examination of each property as it declines or increases within the mixed layer or halocline specifically, and with respect to the full 150m of the water column. To show general trend behavior, least-squares linear trend lines are fitted to the observational data represented in the full column. Figure 9 shows the individual data points, from individual profiles, that fall within seasonal and spatial constraints, and illustrates the least-squares fit as applied in the study. For the remainder of plots shown, the raw data points will not be depicted (for clarity of display), however the trends continue to be fitted to those values. Also for clarity, trend lines are not displayed for the Sfc-MLD and MDL-150m layer values, however the behavior in these layers is shown by the plotted vertical integrals and averages for each winter season (color coded as shown in Figure 5, and 10–16).

Statistical significance is evaluated for all trends based on a 95% Confidence Interval, as summarized in Table 1. Except for the MLD in the Beaufort Shelf data set, there are statistically significant 34-year trends for all parameters/all regions.
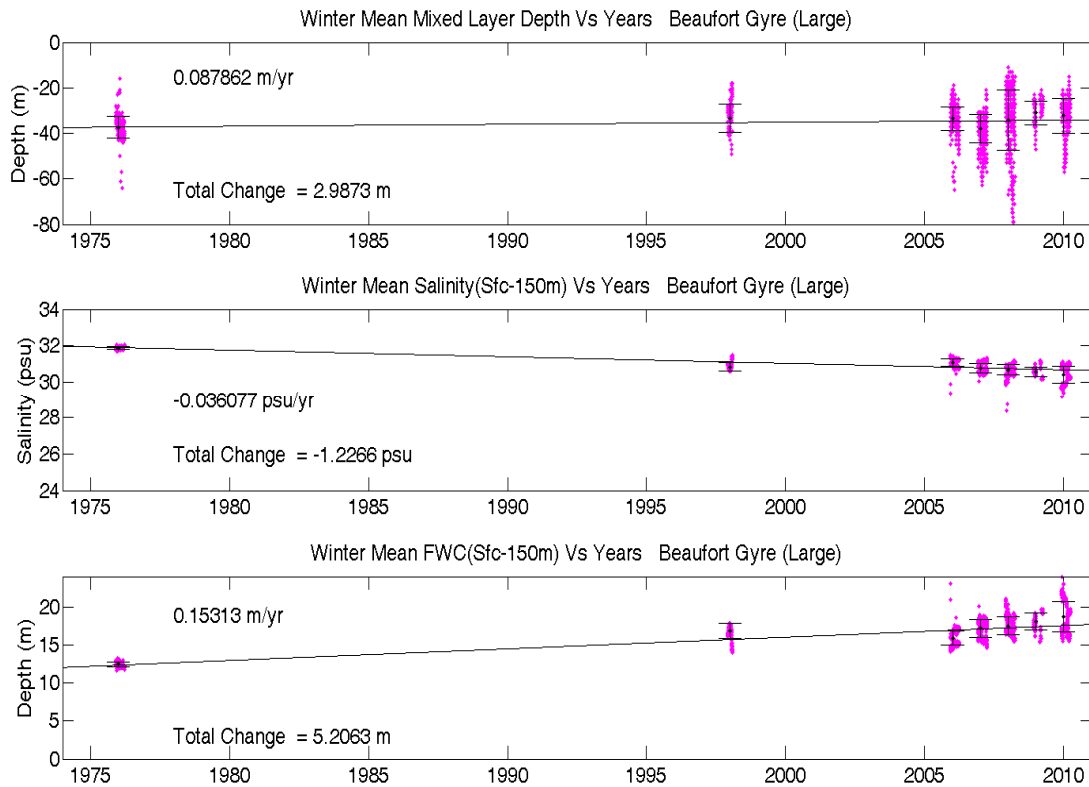
Figure 9.   Beaufort Gyre (Large) Trends. Top Panel: Mixed Layer Depth. Mid-Panel: Salinity (Sfc-150m). Lower Panel: Fresh Water Content (Sfc-150m). Magenta colored dots show the original individual data points from the observations for each winter season (Dec/Jan/Feb/Mar). Black line is linear fit to the original Sfc-150m data points.

1.   Beaufort Gyre

The two Beaufort Gyre sub-regions (large and small) show similar qualitative trends for all variables, with some quantitative differences in steepness between the areas. Figures 10–11 (Large Gyre) and 12–13 (Small Gyre) demonstrate the 34-year evolution for these areas.

Large/Small Gyre MLD: Figure 10–13, all top panels, illustrate MLD. In the large gyre, MLD has a statistically significant shoaling of ~3m over the period, and the small gyre shoals by ~2.5m in total. While these calculated trends are statistically

significant (see Table 1), there is not a significant physical evolution of these bodies of water in terms of MLD change; the 2.5 to 3m changes with respect to the ~40m average MLD in the wintertime means there is less than a 10% change in mixed layer thickness over the 3+ decades. This seems unlikely to be an effect that influences the evolution of freshness and heat within this layer.

Large Gyre S/FWC: In Figure 10, Salinity trends for the three large gyre layers (middle panel) show a relatively small long-term change in the halocline (green), where it drops by ~1 psu over 34 years; there is a larger signal within the mixed layer (blue), where it drops by ~4 psu over the 3+ decades. Fresh Water Content (bottom panel) accumulates in both layers with slightly less total appreciation in the mixed layer, and slightly more within the halocline. Specifically, the mixed layer gains ~2.3m of FWC over the three decades, while the halocline gains ~2.9 meter, resulting in a total of ~5.2m FWC accumulation over 34 years for the entire 150m upper ocean water column (black), or approximately 0.15m/yr).

It should be noted that there is a strong disparity in total depth representation by layer; the mixed layer being ~40m thick (wintertime average) most of the time, while the MLD-150m layer (halocline) occupies nearly 75% of the total 150m column. This depth inequality is relevant for all variables. For example the relatively small observed change in halocline salinity results in a FWC increase that is comparable to that seen in the mixed layer.

Small Gyre S/FWC: In Figure 12, Salinity trends within the three layers are similar to the large Gyre area, with a smaller trend signal in the halocline and a more rapidly evolving signal in the mixed layer. Here, mixed layer salinity drops by ~4.5 psu over the three decades. FWC shows larger increases for both layers, and this sub-region indicates greater total accumulation in the mixed layer vs. the halocline (opposite of the relationship in the large gyre). Here, ~3.8m of total Fresh Water Content accumulates in the mixed layer, or ~0.11m/y, and the halocline shows total FWC accumulation of ~3.4m, or ~0.10m/yr. Over the 150m column, there is ~7.2m FWC total accumulation, or ~0.21m/yr. This is ~1.5 times greater than the large gyre annual rate.

Large Gyre DFFP/HC: In Figure 11, Layer-averaged temperature departure from freezing (middle panel) shows a mixed layer that remains near the freezing point over the analysis time span as expected due to the mixed layer being in contact with sea ice during the winter in this region. The halocline shows a 0.41 deg C total increase over the period. Heat Content (bottom panel) evolution therefore takes place almost entirely in the halocline, where the accumulation is ~130 MJ/m^2 (~3.8 MJ/m^2/yr).

Small Gyre DFFP/HC: In Figure 13, Layer-averaged temperature departure from freezing differs from the large gyre such that the halocline shows a larger 0.52 deg C total increase over the period, with a corresponding Heat Content accumulation of ~250 MJ/m^2 (~7.4 MJ/m^2/y).

Figure 10.   Beaufort Gyre (Large) Freshening Trends. Top Panel: Mixed Layer Depth. Mid-Panel: 3-Layer Salinity Averages. Lower Panel: 3-Layer Fresh Water Content Averages. Color Code: Sfc-MLD = Green, MLD-150m = Blue, Sfc-150m = Black. Black line is linear fit to the original Sfc-150m data points.

28
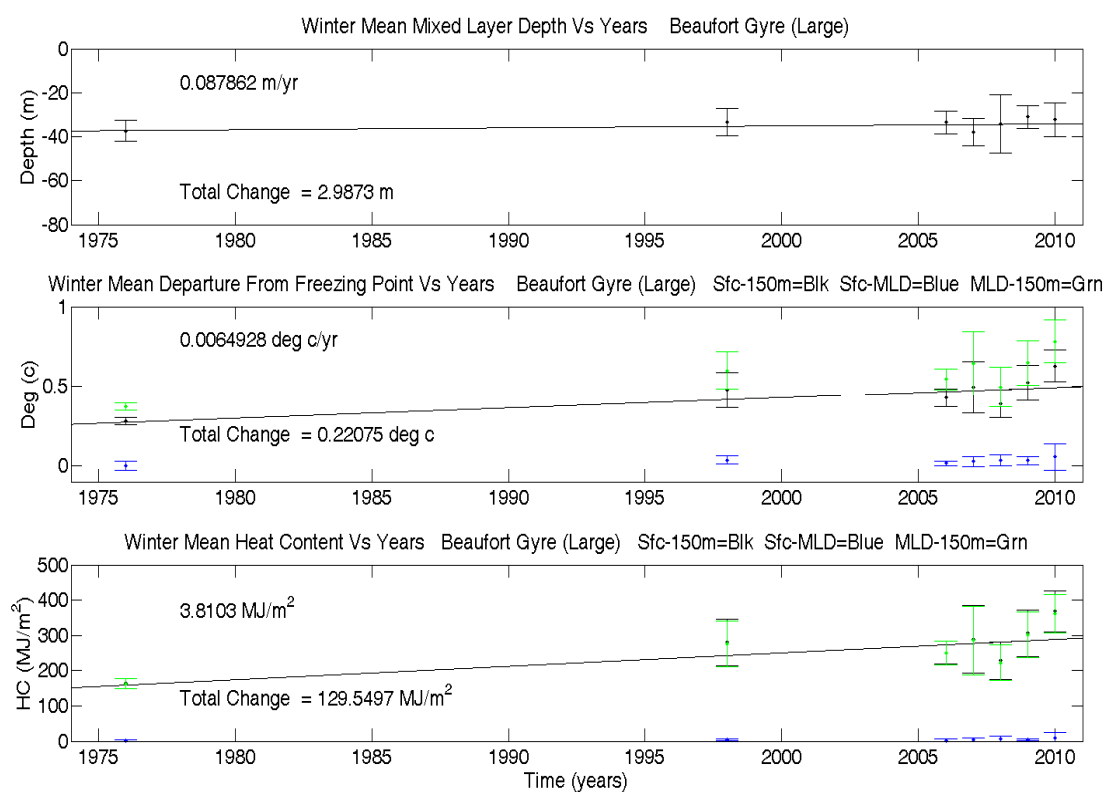
Figure 11.   Beaufort Gyre (Large) Heat Content Trends. Top Panel: Mixed Layer Depth. Mid-Panel: 3-Layer Departure From Freezing Averages. Lower Panel: 3-Layer Heat Content Averages. Color Code: Sfc-MLD = Green, MLD-150m = Blue, Sfc-150m = Black. Black line is linear fit to the original Sfc-150m data points.
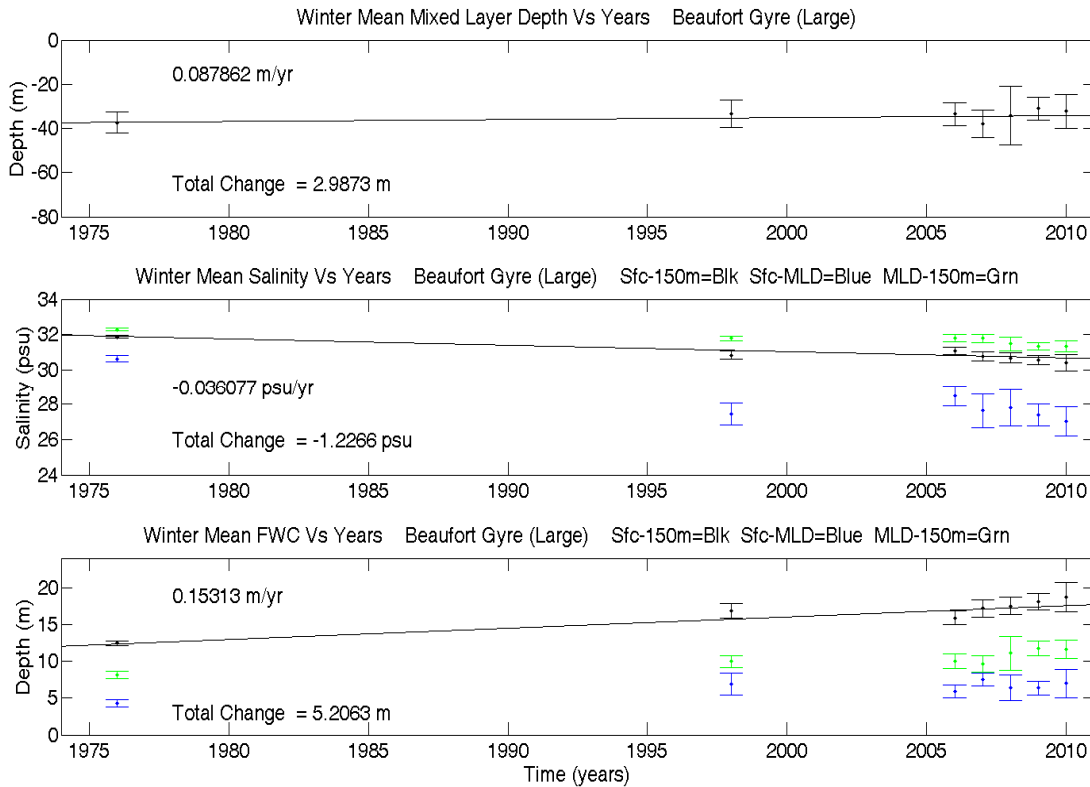
Figure 12.   Beaufort Gyre (Small) Freshening Trends. Top Panel: Mixed Layer Depth. Mid-Panel: 3-Layer Salinity Averages. Lower Panel: 3-Layer Fresh Water Content Averages. Color Code: Sfc-MLD = Green, MLD-150m = Blue, Sfc-150m = Black. Black line is linear fit to the original Sfc-150m data points.
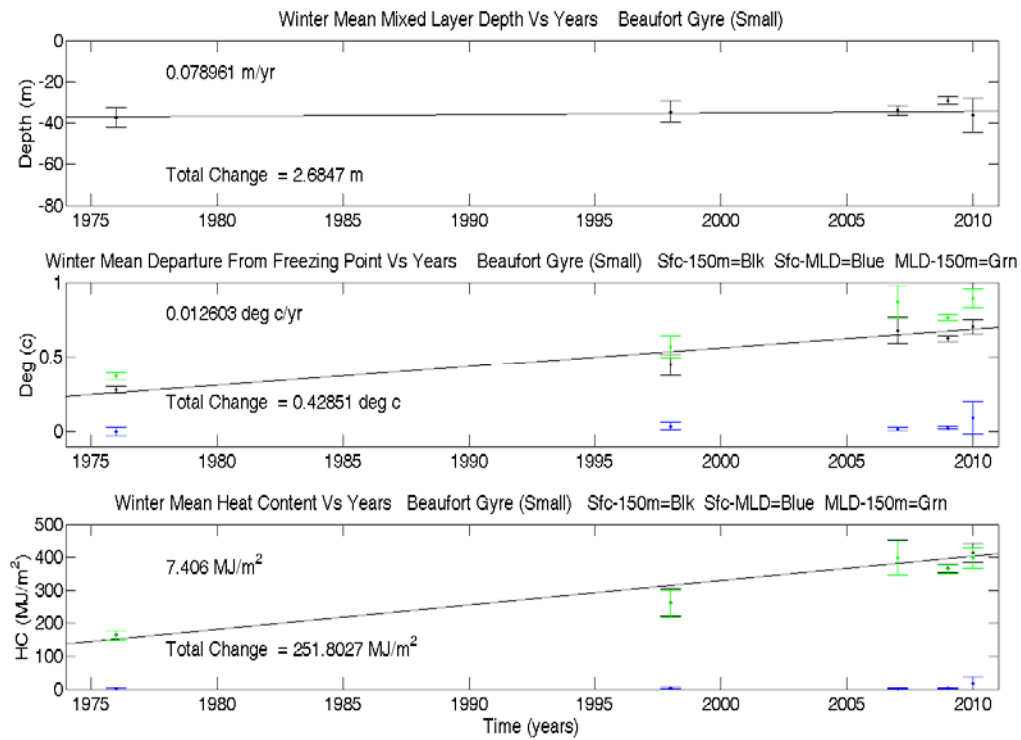
Figure 13.   Beaufort Gyre (Small) Heat Content Trends. Top Panel: Mixed Layer
Depth. Mid-Panel: 3-Layer Departure From Freezing Averages. Lower
Panel: 3-Layer Heat Content Averages. Color Code: Sfc-MLD = Green,
MLD-150m = Blue, Sfc-150m = Black. Black line is linear fit to the
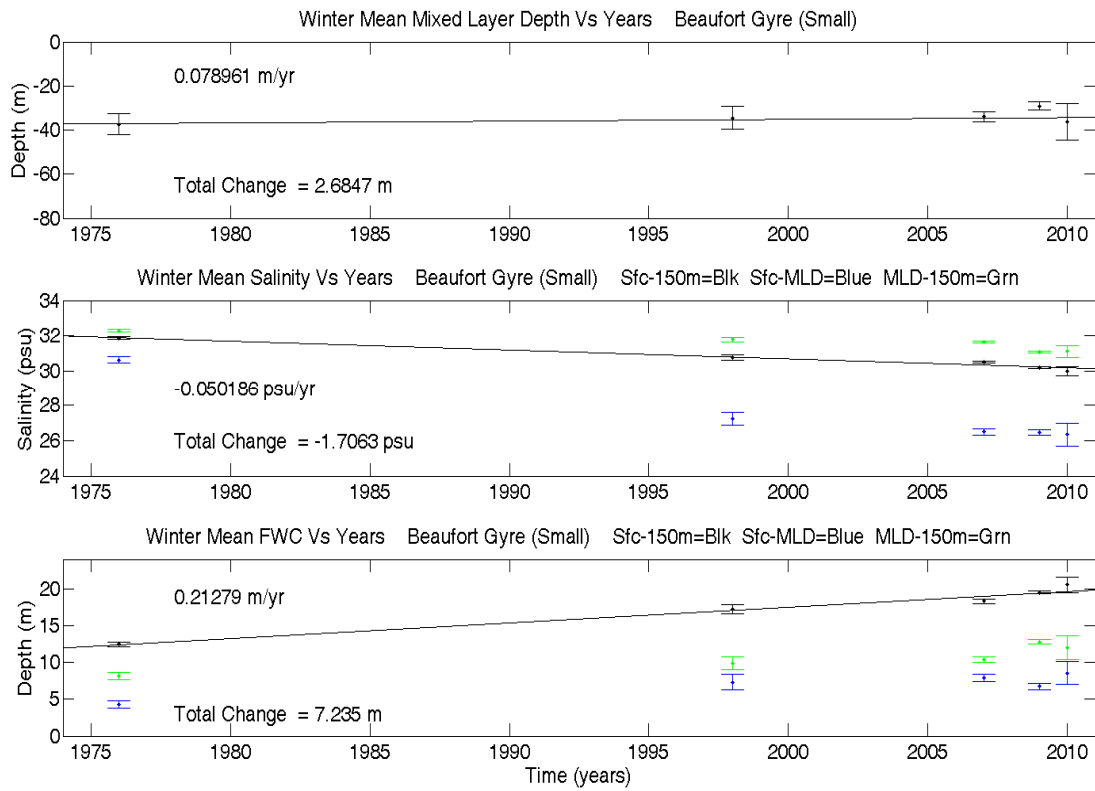original Sfc-150m data points.

2.   Beaufort Shelf

The Beaufort Shelf trends are of the same nature as the BG trends for all
parameters. Here, no change in MLD was detected (slope was not statistically different
than zero). For the other variables, it was not anticipated that trend steepness would be
this similar given that the area was chosen to represent a different hydrographic regime.
This is an area of shallower waters in close proximity to a major river out-flow point (the
mouth of the Mackenzie River). In this area, mixed layer salinity declines very similarly
to the large gyre (not as steeply as the small gyre). FWC accumulates slightly faster here
than in the large gyre, but not on pace with the small gyre. Heat content accumulates
very similarly to the large gyre rate. See Figures 14–15.

31

Figure 14.   Beaufort Shelf Freshness Trends. Top Panel: Mixed Layer Depth. Mid-Panel: 3-Layer Salinity Averages. Lower Panel: 3-Layer Fresh Water Content Averages. Color Code: Sfc-MLD = Green, MLD-150m = Blue, Sfc-150m = Black. Black line is linear fit to the original Sfc-150m data points.
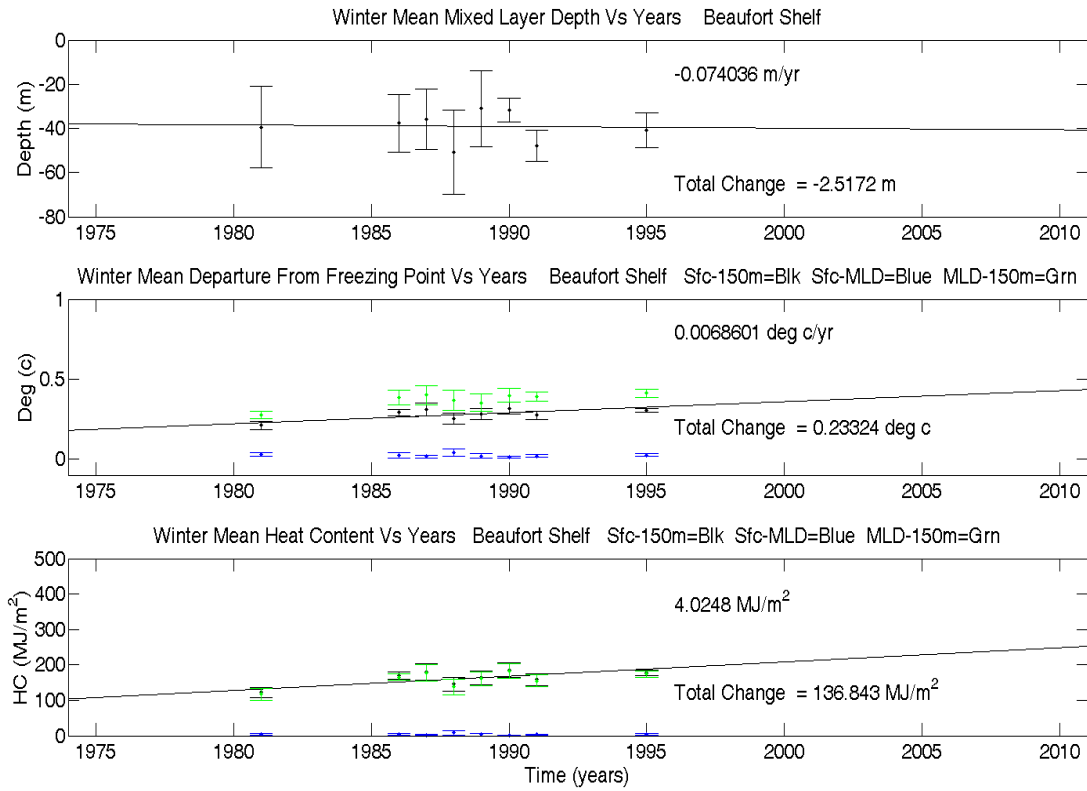
Figure 15.   Beaufort Shelf Heat Content Trends. Top Panel: Mixed Layer Depth. Mid-Panel: 3-Layer Departure From Freezing Point Averages. Lower Panel: 3-Layer Heat Content Averages. Color Code: Sfc-MLD = Green, MLD-150m = Blue, Sfc-150m = Black. Black line is linear fit to the original Sfc-150m data points.

3.   Trans Polar Drift

The collected archive for this sub-region of the Arctic contained an insufficient span of years to estimate long- term trends for this study. Figure 16 demonstrates that only three winters were available in the observational record, and that the trends calculated cannot be interpreted with confidence and perhaps are not realistic as well.
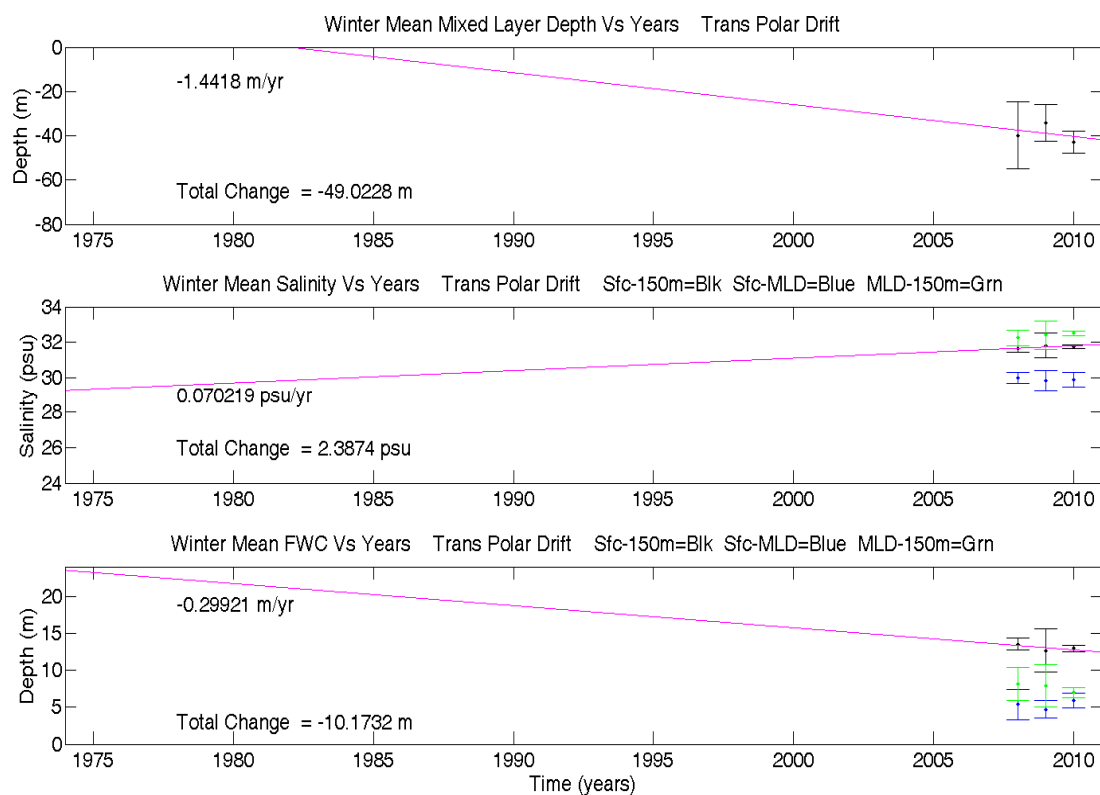
Figure 16.   Trans Polar Drift (Central Arctic) Freshening Trends. Top Panel: Mixed
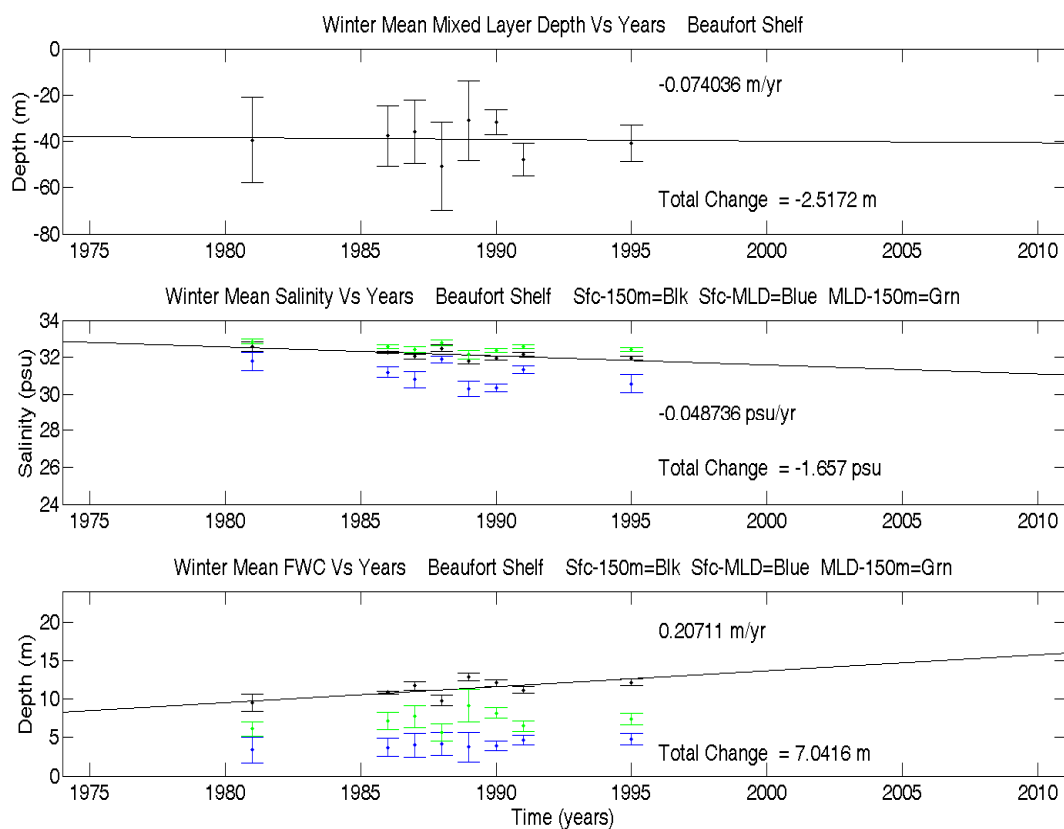Layer Depth. Mid-Panel: 3-Layer Salinity Averages. Lower Panel: 3-Layer
Fresh Water Content Averages. Color Code: Sfc-MLD = Green, MLD-
150m = Blue, Sfc-150m = Black. Magenta line is linear fit to the original
Sfc-150m data points (trends not valid).

B.   SUMMARY MATRIX

	BG (Large)	BG (Small)	Shelf
MLD (m/yr)	+ 0.085 ± 0.032	+ 0.068 ± 0.025	Trend Not Resolved
S (psu/yr)	- 0.036 ± 0.001	- 0.050 ± 0.0009	- 0.049 ± 0.014
FWC (m/yr)	+ 0.153 ± 0.006	+ 0.213 ± 0.004	+ 0.207 ± 0.058
DFFP (deg C/yr)	+ 0.006 ± 0.0005	+ 0.012 ± 0.0004	+ 0.007 ± 0.0021
HC MJ/m^2/yr	+ 3.81 ± 0.293	+ 7.41 ± 0.210	+ 4.02 ± 1.260

Table 1.   34 Year Trends for Sfc-150m Vertical Integrals and Averages: Variables and Sub-regions are: Mixed Layer Depth (MLD) in m/yr, Salinity (S) in psu/yr, Fresh Water Content (FWC) in m/yr, Departure From Freezing Point (DFFP) deg C/yr, and Heat Content (HC) in MJ/m^2/yr. Beaufort Gyre (BG), large and small, and Beaufort Shelf ("Shelf"). Statistical Confidence Intervals based on 95% confidence.

THIS PAGE INTENTIONALLY LEFT BLANK

VI. DISCUSSION

A. GENERAL SUMMARY

In this study, sparse CTD profile observations were used to establish upper ocean trends in heat and freshness over a three decade span. The freshness trends meet expectations with respect to previous investigations and are consistent with sea ice melt and river runoff records. The heat trends are consistent with records of recent increases in the amount of Pacific water advection through the Bering Strait as discussed in Chapter II-B-3. When being compared with other experiments, results from this thesis are hereafter referred to as NPS10; McPhee et al. (1998) is hereafter referred to as M98.

1. Considerations About the Beaufort Gyre Trends

The general NPS10 FWC increase of ~0.15m/yr, in the NPS10 large gyre, bears some resemblance to the M98 approximation made in the late 1990s regarding the disparity between SHEBA and AIDJEX, as they estimated ~2m FWC increase over ~20 years, or ~ 0.1m/yr. The general consistency suggests that the mechanisms driving this change are continuing to work in a similar manner, and the slightly higher rate shown in NPS10 suggests that a steepening of the FWC accumulation rate may have occurred sometime since the 1990s, near or after the M98 data set. In this study no effort is made to decipher breaking-points in trend steepness on a decade to decade basis because the data set employed does not lend itself to that type of scrutiny. A more comprehensive data set (in terms of missing blocks of years) might have enabled a higher order fit in the trend curves, but the gaps between expeditions and camps negates this opportunity. The implied change in steepness is, however, consistent with a similar investigation where by Proshutinsky et al. (2009) suggests an increase in the freshening rate of the Beaufort Gyre beginning near the early 2000s. Proshutinsky et al. (2009) is hereafter referred to as P09.

If the very general approximation is made that sea ice is mostly fresh, the FWC accumulation over time can be related to the loss in sea ice thickness as shown in Figure 2, from Kwok et al. (2009). In this relationship, the loss of thickness is on the order of a few meters over ~4 decades, which bears some resemblance to the gain of a few meters of FWC in the upper ocean over a similar time-frame. This crude correlation has value in that the direction of the two trends meets perfectly with the expected qualitative relationships between these parameters, assuming that the sea ice melt water is retained within the gyre.

With respect to the disparity in the FWC accumulation rates of the NPS10 larger vs. smaller BG areas, there is also consistency with the P09 findings. The annual NPS10 small gyre rate of 0.21m/yr vs. 0.15m/yr in the large gyre implies a difference in relationship to the center of the gyre. In consideration of Figure 17, the center position of the gyre has tended to be very near the locations of a set of hydrographic profiler moorings (A, B, C and D) over the past two decades – this is in the vicinity of ~78N 150W. This position is within a few hundred kilometers of the center point of the NPS10 small and large gyre sub-regions. Because the gyre center is migratory, it is difficult to estimate exactly where it was during the observation periods and its influence is a matter of conjecture.
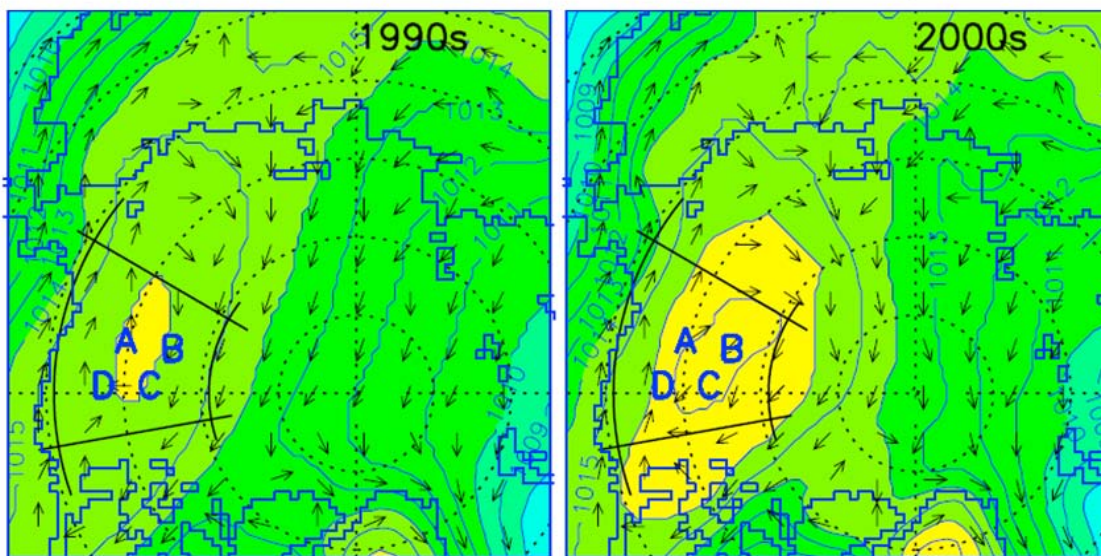
Recent Position of the Beaufort Gyre

Figure 17.   Annual Sea Level Pressure (hPa) (Solid contour lines and color shades) and geostrophic wind direction (vector arrows) for the 1990s and 2000s. A, B, C, and D depict locations of hydrographic profiler moorings near the center position of the Beaufort Gyre during this period. (From Proshutinsky et al. 2009).

There are two important considerations in view of the center position of the gyre: (1) the wind fields from the 70s and 80s indicate the center was most likely located at higher meridians, e.g., 165-170W or so, over the North Wind Rise/edge of the Chukchi Sea, but at roughly the same latitude, and (2) the P09 experiment indicates that the strongest FWC accumulation occurs near the center of the gyre, with a "tapering away" effect as you move outward from the center. This implies that some portion of the stronger FWC signal (in both large and small gyres) near the end of the NPS10 34 year span may be influenced by the relocation of the gyre, such that it brought stronger accumulation characteristics into the vicinity of the centers of the NPS10 sub-regions. The stronger signal in the small gyre may be an indication that it provides a better representation of the characteristics near the center, while the large gyre somewhat represents the whole expanse of the gyre. This aspect of the small gyre may also explain its faster accumulation of heat as compared to the large gyre area.

39

Disparities between FWC accumulations in the mixed layer vs. the halocline indicate possible changes in the importance of different contributors. Due to the separation of the mixed layer from the halocline below, by a large density difference across the base of the mixed layer in the open waters of the NPS10 BG sub-regions, the general expectation is that mixed layer trends and halocline trends have unique drivers. This estimation is made with awareness that there are some exceptions. It is estimated that newly added fresh water is contributed to the mixed layer by sea ice melt water and river runoff, while the FWC contribution in the halocline seems to mainly result from advection at depth. While sea ice melt water goes immediately into the mixed layer (during the melt seasons) over all ocean regions that have ice cover, the river runoff typically has a residence time along the shelf areas before it becomes part of the open ocean Arctic waters.

If detailed chemical analyses accompanied these CTD data sets, more detail could be revealed, but very few of the observations in this archive database were taken coincidentally with bottle samples. The fact that the mixed layer, while representing less than $1/4^{th}$ of the water column, accumulated approximately 40% of the FWC gained over the three decades is indicative that the near surface contributors (river runoff and sea ice melt water) are especially important. The trend implies that the melt water and/or river runoff contribution is becoming an increasingly important influence in terms of percent share of the total FWC budget in the upper ocean. This interpretation, and the general interpretation that NPS10 mixed layer freshening is significantly driven by melt water, is consistent with recent increases in the rate of observed sea ice decline as discussed in Kwok et al. (2009) and Stroeve et al. (2007), and ocean chemical analysis work as discussed in Yamamoto- Kawai (2009). The interpretation that pacific advection is responsible for the NPS10 freshening halocline is consistent with the Woodgate et al. (2010) findings on Bering Strait Arctic bound flow rates in recent years. This consistency also exists with respect to the NPS10 MLD-150m increasing Heat Content trends.

2. Comparison of the Beaufort Gyre to the Beaufort Shelf

As the trends were so similar to the large gyre, it is difficult to identify mechanisms of influence that are unique to the NPS10 shelf area. The proximity to the mouth of the Mackenzie River might lend expectation for a near surface FWC signal related to the general increase in discharge from rivers in the Arctic system, as discussed by Peterson and colleagues (2002). The very slight difference in FWC increase on the shelf vs. the large gyre could be related to the Mackenzie River, however this difference is very small, and the trend may simply be part of the general FWC increase taking place in much of the Canada Basin. The same seems to be the case with heat content as the trend rate is such a close resemblance to the large gyre. The specific constraints placed on the Shelf region data set, allowed for some of the observations to be basin-ward of the shelf break by a few tens of kilometers in some cases (so as to include all the original ship-borne observations in this data set, and maximize the sample size), while most of the observations were in shelf waters. Another examination with smaller spatial constraints (strictly shelf locations) might have helped in identifying characteristics unique to the shelf regime; however, this would have reduced sample size, and perhaps affected confidence in the trends.

B. NEW TECHNOLOGIES AND REGIONAL OUTLOOK

During the time-span of the data set used for this study, technology has gone from expensive, manned ice-camps to autonomous instruments profiling with significantly greater spatial and temporal coverage. While field work efforts like AIDJEX and SHEBA provided critical glimpses into the Arctic "big picture", a key take-away from those experiences was to realize the need for more data coverage in both space and time. These insights lead to the development of the new systems like the WHOI ITPs, ice mass balance buoys and autonomous ocean flux buoys that can be deployed within the Arctic Basin for year+ intervals at a small fraction of the cost of manned ice camps. Having had these types of data sources available for several years now has vastly improved the abilities of the scientific community to make estimates of hydrographic properties and trends, and it will continue to be essential to make advancements in these automated observational systems and networks as the environment continues to change.

THIS PAGE INTENTIONALLY LEFT BLANK

LIST OF REFERENCES

Arnell, N.W., 2005: Implications of climate change for freshwater inflows to the Arctic Ocean. *Journal of physical Research*, **110**. D07105.

Bush, G.W., President of the United States, 2009: National Security Presidential Directive - 66.

Col, S., 2010: Fine-scale variability in temperature, salinity, and pH in the upper-ocean and the effects on acoustic transmission loss in the western arctic ocean. Department of Oceanography, Naval Postgraduate School, 107 pp.

Hanson, K. J., 1961. The Albedo of Sea ice and Ice Islands in the Arctic Ocean Basin. *Arctic*, **14**, 188–196.

Kwok, R., and Rothrock, D.A., 2009: Decline in Arctic sea ice thickness from submarine and ICESat records: 1958–2000. *Geophysical Research Letters*, **36**, L15501.

Kwok, R., Cunningham, G.F., Wensnahan, M., Rigor, I., Zwally, H.J., and Yi, D., 2009: Thinning and volume loss of the Arctic Ocean sea ice cover: 2003–2008: *Journal of Geophysical Research*, **114**, C07005.

Laine, V., 2004: Arctic sea ice regional variability and trends, 1982–1998. *Journal of Geophysical Research*, **109**. C06027.

Lindsay, R.W., Zhang, J., Schweiger, M., Steele, M., and Stern, H., 2009: Arctic Sea Ice retreat in 2007 Follows Thinning Trend: *Journal of Climate*, **22**, 165–176.

Markus, T., Stroeve, J.C., and Miller, J., 2009: Recent changes in Arctic sea ice melt onset, freezup, and melt season length. *Journal of Geophysical Research*, **114**. C12024.

McPhee, M.G., and Stanton, T.P., 1998: Freshening of the upper ocean in the Arctic: Is perennial sea ice disappearing? *Geophysical Research Letters*, **25**(10), 1729–1732.

McPhee, M.G., Proshutinsky, A., Morrison, J. H., Steele, M., and Alkire, M.B., 2009: Rapid change in freshwater content of the Arctic Ocean. *Geophysical Research Letters*, **36**, L10602.

National Snow and Ice Data Center, cited 2010: CTD Data Set: Beaufort Sea Cruises and Ice Stations, and North Water Polynya Aircraft Surveys. [Available online at http://nsidc.org/data/arctic_ocean_expeditions/ctd/melling2eh.html.]

Perovich, D.K., 2005: On the aggregate-scale partitioning of solar radiation in Arctic sea ice during the Surface Heat Budget of the Arctic Ocean (SHEBA) field experiment. *Journal of Geophysical Research*, **110**. C03002.

Perovich, D.K., Nghiem, S.V., Markus, T., and Schweiger, A., 2007: Seasonal evolution and interannual variability of the local solar energy absorbed by the Arctic sea ice-ocean system. *Journal of Geophysical Research*, **1124**, C03005.

Peterson, B.J., Holmes, R.M., McClelland, J.W., Vorosmarty, C.J., Lammers, R.B., Shiklomanov, A.I., Shiklomanov, I.A., and Rahmstorf, S., 2002: Increasing River Discharge to the Arctic Ocean. *Science*, **298**. 2171-2173.

Proshutinsky, A., Krishfield, R., Timmermans, M-L., Toole, T., Carmack, E., McLaughlin, F., Williams, .J., Zimmermann, S., Itoh, M., and Shimada, K., 2009: Beaufort Gyre freshwater reservoir: State and variability from observations. *Journal of Geophysical Research*, **114**, C00A10.

Serreze, M.C., Barrett, A.P., Slater, A.G., Woodgate, R.A., Aagaard, K., Lammers, R.B., Steele, M., Moritz, R., Meredith, M., and Lee, C.M., 2006: The large-scale freshwater cycle of the Arctic. *Journal of physical Research*, **111**. C11010.

Stroeve, J., Holland, M.M., Meier, W., Scambos, T., Serreze, M., 2007: Arctic sea ice decline: Faster than forecast. *Geophysical Research Letters*, **34**, L09501.

Task Force Climate Change / Oceanographer of the Navy, 2009: Navy Arctic Roadmap.

Task Force Climate Change / Oceanographer of the Navy, 2009: Navy Climate Change Roadmap.

Woodgate, R.A., Weingartner, T., and Lindsay, R., 2010: The 2007 Bering Strait Ocean Heat Flux and anomalous Arctic Sea-ice Retreat. *Geophysical Research Letters*, **37**. L01602.

Woods Hole Oceanographic Institute, cited 2010: Ice Tethered Profiler. [Available online at http://www.whoi.edu/page.do?pid=20756.]

Yamamoto-Kawai, M., McLaughlin, F.A., Carmack, E.C., Nishino, S., Shimada, K., and Kurita, N., 2009: Surface freshening of the Canada Basin, 2003–2007. *Journal of Geophysical Research*, **114**, C00A05.

INITIAL DISTRIBUTION LIST

1. Defense Technical Information Center
    Ft. Belvoir, Virginia

2. Dudley Knox Library
    Naval Postgraduate School
    Monterey, California

3. Tim Stanton
    Naval Postgraduate School
    Monterey, California

4. Bill Shaw
    Naval Postgraduate School
    Monterey, California

5. CAPT Jim Pettigrew, USN
    Fleet Numerical Meteorology and Oceanography Center
    Monterey, California